Wide diversity of *PAX5* alterations in B-ALL: a Groupe Francophone de Cytogénétique Hématologique study

*Etienne Coyaud,[1,2] *Stephanie Struski,[3] Nais Prade,[1] Julien Familiades,[1,2] Ruth Eichner,[1,2] Cathy Quelen,[1,2] Marina Bousquet,[1,2] Francine Mugneret,[4] Pascaline Talmant,[5] Marie-Pierre Pages,[6] Christine Lefebvre,[7] Dominique Penther,[8] Eric Lippert,[9] Nathalie Nadal,[10] Sylvie Taviaux,[11] Bruce Poppe,[12] Isabelle Luquet,[13] Laurence Baranger,[14] Virginie Eclache,[15] Isabelle Radford,[16] Carole Barin,[17] Marie-Joëlle Mozziconacci,[18] Marina Lafage-Pochitaloff,[19] Hélène Antoine-Poirel,[20] Christiane Charrin,[21] Christine Perot,[22] Christine Terre,[23] Pierre Brousset,[3] Nicole Dastugue,[3] and Cyril Broccardo[1]

[1]Inserm, U563, Toulouse, France; [2]Université Toulouse III Paul Sabatier, Centre de Physiopathologie Toulouse Purpan, Toulouse, France; [3]Centre Hospitalier Universitaire (CHU) Toulouse, Department of Hematology, Toulouse, France; [4]CHU Le Bocage, Dijon, France; [5]CHU Nantes, Nantes, France; [6]CHU Lyon Sud, Pierre benite, Lyon, France; [7]CHU Grenoble, Grenoble, France; [8]Centre de lutte contre le cancer Henri Becquerel-Rouen, France; [9]CHU Bordeaux, Pessac, France; [10]CHU Hôpital Nord, St Etienne, France; [11]CHU Montpellier, Montpellier, France; [12]Ghent University Hospital, Ghent, Belgium; [13]CHU Reims, Reims, France; [14]CHU Angers, Angers, France; [15]CHU-Hôpital Avicenne, Bobigny, France; [16]CHU Necker, Paris, France; [17]CHU Bretonneau, Tours, France; [18]Institut Paoli Calmettes, Marseille, France; [19]CHU Timone, Marseille, France; [20]Cliniques Universitaires St-Luc, Bruxelles, Belgium; [21]CHU Lyon, Lyon, France; [22]Hôpital Saint-Antoine, Paris, France; and [23]Centre hospitalier de Versailles, Le Chesnay, France

***PAX5* is the main target of somatic mutations in acute B lymphoblastic leukemia (B-ALL). We analyzed 153 adult and child B-ALL harboring karyotypic abnormalities at chromosome 9p, to determine the frequency and the nature of *PAX5* alterations. We found *PAX5* internal rearrangements in 21% of the cases. To isolate fusion partners, we used classic and innovative techniques (rolling circle amplification-rapid amplification of cDNA ends) and single nucleotide polymorphism-comparative genomic hybridization arrays. Recurrent and novel fusion partners were identified, including *NCoR1*, *DACH2*, *GOLGA6*, and *TAOK1* genes showing the high variability of the partners. We noted that half the fusion genes can give rise to truncated PAX5 proteins. Furthermore, malignant cells carrying *PAX5* fusion genes displayed a simple karyotype. These data strongly suggest that *PAX5* fusion genes are early players in leukemogenesis. In addition, *PAX5* deletion was observed in 60% of B-ALL with 9p alterations. Contrary to cases with *PAX5* fusions, deletions were associated with complex karyotypes and common recurrent translocations. This supports the hypothesis of the secondary nature of the deletion. Our data shed more light on the high variability of *PAX5* alterations in B-ALL. Therefore, it is probable that gene fusions occur early, whereas deletions should be regarded as a late/secondary event. (*Blood*. 2010;115(15):3089-3097)**

Introduction

Precursor B-cell acute lymphoblastic leukemia (B-ALL) is characterized both by a blockage of B-cell differentiation and uncontrolled proliferation of blastic cells. Adult and childhood B-ALL differs in terms of prognosis.[1] Although 80% of children with ALL can be cured, only 30% of adults achieve long-term disease-free survival.[1] These discrepancies in prognosis correlate with different occurrences of chromosomal abnormalities. Besides frequent recurrent translocations, such as t(9;22)(q34;q11), t(12;21)(p13;q22), t(1;19)(q23;p13), or *MLL* translocation, new oncogenes have been identified recently. Among them, the paired box domain gene 5 (*PAX5*), located on 9p13, has been reported as being frequently mutated in both childhood[2] and adult B-ALL.[3]

PAX5 encodes a paired box domain (PBD) transcription factor considered as the guardian of B-cell identity. Its homozygous deletion in the mouse leads to total blockage of B-cell differentiation at the pro-B stage.[4] Furthermore, *Pax5* inactivation at later stages of differentiation entails transdifferentiation or dedifferentiation of B cells.[5] Pax5, which activates crucial genes for B-cell lineage differentiation and represses genes important for commitment in other hematopoietic lineages, is expressed from early pro-B stage until final plasmacytic differentiation, where it is turned off.[6,7]

Fusion genes involving *PAX5* have been associated with blockage of B-cell differentiation, the first reported example being *PAX5-ETV6*, the product of the dic(9;12)(p13;p13) rearrangement.[8] A recent study has shown that *PAX5* is rearranged in 2.6% of pediatric B-ALL cases,[9] being fused, to date, with 17 different partners, thus demonstrating the variability of the fusion partners. In contrast, very few studies have been performed on adult B-ALL, only reporting fusion between *PAX5* and *ETV6*[10] and the elastin gene (*ELN*).[11] Cytogenetic abnormalities affecting the chromosome 9p arm and potentially involving *PAX5* occur in 10% of child B-ALL.[12] Using classic cytogenetic techniques and a newly developed molecular strategy (rolling circle amplification-rapid amplification of cDNA ends [RCA-RACE]), we investigated 9p abnormalities, focusing especially on the *PAX5* locus. For this

Submitted July 27, 2009; accepted January 22, 2010. Prepublished online as *Blood* First Edition paper, February 16, 2010; DOI 10.1182/blood-2009-07-234229.

The online version of this article contains a data supplement.

The publication costs of this article were defrayed in part by page charge payment. Therefore, and solely to indicate this fact, this article is hereby marked "advertisement" in accordance with 18 USC section 1734.

*E.C. and S.S. contributed equally to this study.

purpose, we collected 153 childhood and adult B-ALL with 9p rearrangements diagnosed and reviewed by members of the Groupe Francophone de Cytogénétique Hématologique (GFCH). Our data revealed that *PAX5* deletions accounted for most of the 9p alterations and were often associated with complex karyotypes. On the contrary, *PAX5* internal rearrangements were less frequent and were most of the time the sole chromosomal abnormality detected. This collaborative study also allowed the description of novel *PAX5*-fusion partners.

Methods

Patients

The criterion for inclusion, in this retrospective study of the GFCH, was the detection by karyotype analysis of acquired structural 9p rearrangement in patients with B-ALL. We selected the structural abnormalities with the largest variety of 9p chromosome partners because the aim of the study was to find new fusion partners of *PAX5*.

This retrospective study included 153 B-ALL (92 males and 61 females) recruited from 1989 to 2008 from 20 French and 2 Belgian cytogenetic centers ("Morphologic and immunologic validation"). Among them, we examined 140 patients at diagnosis and 13 at relapse. This cohort was composed of 89 children (median age, 6 years; range, 1 month to 15 years, 52 males and 37 females) and 64 adults (median age, 43 years; range, 16-82 years, 40 males and 24 females). Patients distributed according to the EGIL classification[13] of B-ALL subtypes were: B-I ALL (n = 6), B-II ALL (n = 92), B-III ALL (n = 48), and B-ALL unclassified (n = 7).

Morphologic and immunologic validation

Morphologic and immunophenotypic studies of patients were carried out in each center and validated by groups of morphologists and immunologists responsible for data collection in various working groups, particularly involved in therapeutic protocols for children (EORTC, FRALLE, and IGLALL) and adults (GOELAL, GRAALL, GRAAPH, LALA, and OMAN). Patient material was provided by participative centers (Centre Hospitalier Universitaire Toulouse, n = 42; Strasbourg, n = 16; Dijon, n = 11; Nantes, n = 11; Lyon, n = 9; Grenoble, n = 8; Rouen, n = 8; Bordeaux, n = 8; St Etienne, n = 7; Montpellier, n = 6; Ghent, Belgium, n = 4; Reims, n = 4; Angers, n = 3; Bobigny n = 3; Paris, Necker, n = 3; Tours, n = 3; Marseille IPC, n = 2; Marseille, Timone, n = 1; Laboratoire Biomnis, Lyon, n = 1; Louvain, Belgium, n = 1; Paris, St Antoine, n = 1; Versailles, n = 1).

Cytogenetics

Cytogenetic analysis was conducted on bone marrow in 139 cases, on peripheral blood in 12 cases, on the central nervous system in 1 case, and on lymph nodes in another. In this multicenter study, different cellular culture techniques were used. Short synchronized cultures (≤ 24 hours) were most frequently carried out. RHG or GTG banding techniques (or both) were applied and karyotypes described according to the International System for Human Cytogenetic Nomenclature 2005.[14] All chromosomal data were reviewed by the members of GFCH during 2 successive workshops to sharpen karyotype interpretation.

FISH approach for the detection of *PAX5* rearrangements

A first screening of all 9p rearrangements was performed with a commercial dual-color *PAX5* probe (Dako Denmark). Direct involvement of *PAX5* was verified using 2 overlapping bacterial artificial chromosome (BAC) clones: RP11-243F8 and RP11-344B23 and exon-specific fosmides G248P85962F9 (exon1) and G248P82268A1 (exon10; CHORI). Positioning of probes relative to *PAX5* is depicted in Figure 1.

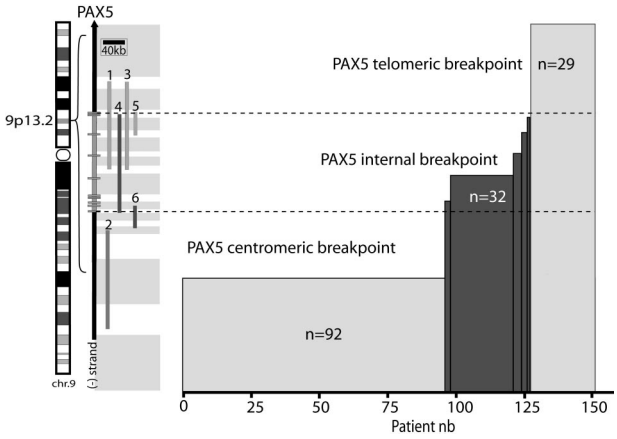

Figure 1. Repartition of breakpoints on chromosome 9p arm. Location of *PAX5* on chromosome 9 (left). A schematic of *PAX5* genomic structure (right); rectangles represent exons. (1-6) Probes used for FISH analyses: telomeric and centromeric Dako commercial probes (1,2), RP11-344B23 (3), and RP11-244F8 (4), BACs and G248P82268A1 (5), and G248P85962F9 (6) fosmids. These probes enable localization of the breakpoint regions (gray rectangles). Histogram represents the number of patients harboring these breakpoints.

PCR approach for the detection of *PAX5* fusion partners

Total RNA was extracted according to the TRIZOL method (Invitrogen) and 1 μg reverse-transcribed into cDNA by SuperScript III (Invitrogen) according to the manufacturer's instructions, using an oligo-dTanchor primer (RACE kit, second generation; Roche Applied Science). The cDNA product was used as a template in a polymerase chain reaction (PCR) experiment performed with the Advantage 2 PCR kit (BD Biosciences), a PCR anchor primer (*5′-GACCACGCGTATCGATGTCGAC-3′*), and the *PAX5*-specific primer *PAX5-771F (5′-CCATGTTTGCCTGGGAGATCAGG-3′*). The temperature cycling program used with a GeneAmp PCR system 9600 (PerkinElmer) was as follows: (1) 1 minute at 94°C; (2) 15 seconds at 94°C, 6 minutes at 68°C 35 times; and (3) 10 minutes at 68°C. A seminested PCR using an internal *PAX5-846F* (*5′-GTTCCATCAACAGGATCATCCGG-3′*) primer and the anchor primer was subsequently performed on 1 μL of the PCR product under the same cycling conditions. The obtained products were sequenced using the *PAX5-846F* primer and BigDye dideoxynucleotides. Products were separated on a 3130 XL sequencing apparatus (Applied Biosystems); electrophoregrams were analyzed using the Sequencher software (Version 4.1.2; Gene Codes Corporation). The presence of chimeric transcripts has been further verified by PCR using specific primers (*PAX5-415F: 5′-CCCTGTCCATTCCATCAAGTCCTG-3′, DACH2-928R: 5′-TGGTTAGCAGGTGGTTCTGCTGC-3′, NCoR1-7605R: 5′-GAGATC-CCTCTCCTGCACCCTG-3′, GOLGA6-2134R: 5′-ACGCAGGGTTTGCT-GGGCAAGC-3′, ELN-2297R: 5′-ATGAGGTCGTGAGTCAGGGGTC-3′, JAK2-4020R: 5′-CACATCTTTGCTGGCTAGCATCATG-3′, FOXP1-2595R: 5′-CAATCTTCATTCTCGGGGTTGG-3′*).

RCA-RACE

Gene-specific RCA was performed as previously described.[15] Briefly, starting from 100 to 250 ng of total RNA, SuperScriptTM III reverse transcription was performed according to the manufacturer's instructions (Invitrogen) replacing the oligo-dT primer by a 5′ phosphate oligo-dT anchor primer (*5′P-GACCACGCGTATCGATGTCGAC$(T)_{16}$V-3′*) at a final concentration of 2.5μM. Circularization of purified cDNA was obtained using CircLigase kit (Epicentre Biotechnologies), according to the manufacturer's instructions. RCA was carried out by mixing the purified circularized product with 5 μL of dNTPs (10 mM each; Promega), 1 μL of 10 mg/mL bovine serum albumin, 5 μL of 10 times ϕ29 DNA polymerase buffer, 10 U of ϕ29 DNA polymerase (New England Biolabs), 2 μL of 100μM *PAX5-Exo5* primer (*5′-CTTGTGATGTTGGCGAGA*A*C - 3′* (*phosphorothiotates chemical bounds, Eurogentec) and water up to 50 μL. This

mixture was incubated for 21 hours at 30°C and then for 10 minutes at 65°C.

Amplification of 50 ng of RCA product was performed with the Advantage 2 PCR kit (BD Biosciences), using *PAX5-771F* and *PAX5-570R* (*5′-ATCCTCTGGCGGACTACATCCG-3′*) primers, according to the manufacturer's instructions. This mixture was incubated under the same cycling condition than for the RACE PCR experiment. If necessary, nested PCR was performed using 1 μL of previous PCR product, replacing *PAX5-771F* by *PAX5-846F* and *PAX5-570R* by *PAX5-510R* (*5′-TTCACTCCTCCATGTC-CTGTCC-3′*) primers. For negative control, the cDNA was replaced by water. For non-B control, cDNA of Karpas cell line, which does not express *PAX5*, was used.

Purification of BAC DNA

BACs (chosen on the website www.genome.ucsc.edu) were amplified in 3 mL LB medium (MP Biomedicals), containing 12.5 μg/mL of chloramphenicol (Sigma-Aldrich) under constant shaking at 180 rpm for 12 hours at 37°C. Each purified BAC DNA was amplified by hyperbranched (H)–RCA: from 20 to 50 ng of BAC DNA was added to 1 μL of exo-resistant random heptamers (Fermentas), 1 μL of annealing buffer (200mM Tris-HCl, pH 8, 50mM $MgCl_2$), and water up to 5 μL. This mixture was incubated for 4 minutes at 94°C on a 2720 Thermal Cycler (Applied Biosystems) and cooled on ice for 2 minutes. Then was added 2 μL of ϕ29 10 times Buffer (New England Biolabs), 1 μL of dNTPs 10mM each (Promega), 7 U of ϕ29 DNA polymerase (New England Biolabs), 0.5 μL of 10 mg/mL bovine serum albumin (New England Biolabs), and water up to 20 μL. This mixture was incubated under the condition described above for gene specific RCA.

Labeling of BAC DNA

BAC DNA was labeled using the nick-translation kit (GE Healthcare) according to the manufacturer's instructions, with dUTP-fluoroscein or dUTP-tetramethylrhodamine (Roche Applied Science). Overnight ethanol precipitation of the labeled DNA was performed in the presence of 0.1 mg of Human Cot-1 DNA (Invitrogen) and 0.2 mg of salmon testis DNA (Sigma-Aldrich). Labeled BAC DNA was then pelleted, dried, and resuspended in 100 μL of a mixture of 50% formamide (Sigma-Aldrich), 2 times SSC (Eurobio), and 10% dextran sulfate (Sigma-Aldrich). BACs are detailed in supplemental Table 1 (available on the *Blood* website; see the Supplemental Materials link at the top of the online article).

CGH array

Genomic DNA was extracted with DNeasy (QIAGEN) from blood or bone marrow samples. Samples were analyzed for copy number changes using Affymetrix Genome-Wide Human SNP 6.0 arrays (Affymetrix). Sample preparation and hybridizations were performed using Genome-wide Human SNP Nsp/Sty assay kit (Affymetrix) according to manufacturer's protocol. Analysis of copy number state was done using BRLMM-P-Plus algorithm with regional GC correction, embedded in Genotyping Console 2.0 software (Affymetrix).

PAX5 vectors

Complete coding sequences of *wtPAX5*, *trPAX5*, and *PAX5-NCoR1* were amplified from cDNA of patient #125, #108, and # 101, respectively, using PfuUltraII Hotstart PCR Master Mix (Stratagene) with primers PAX5-forward: *ATGGATTTAGAGAAAAATTATCCG* and *PAX5*-reverse: *ATGGGCTCTCTGGCTATCTTCAGG* for wtPAX5; *PAX5*-forward and *trPAX5*-reverse: *AGTCTCACCCTGCTGCCTGTCTG* for *trPAX5*; and *PAX5*-forward and *NCoR1*-reverse: *GAGATCCCTCTCCTGCACCCTG* for *PAX5-NCoR1*. PCR products were cloned into pcDNA3.1 (+) expression vector (Invitrogen)

Luciferase assay

Experiments had been performed as previously described[11] replacing *pRenilla-CMV* by *pSV-β-galactosidase* (Promega) as transfection efficiency reporter plasmid. HeLa cells (in 6-well plates) were transfected with 1.5 μg *luc-CD19*,[16] 1.5 μg *pSV-β-galactosidase*, 0.3 μg *pcDNA3-PAX5*, and increasing amounts of *pcDNA3-truncated PAX5* or *pcDNA3-PAX5-NCoR1* (0.1-0.9 μg). Luciferase and β-galactosidase activity were revealed on a Mithras LB940 (Berthold Technologies) using Luciferase Reporter assay system and β-galactosidase enzyme assay system, respectively (Promega). Luminescence and absorbance were read by a Mithras LB940 (Berthold Technologies).

Firefly luciferase activity was normalized to the measured β-galactosidase activities and are shown as average values relative to the basal activity observed with *pcDNA3* alone (mean ± SD); statistical significance of normalized luciferase activity was assessed by Wilcoxon Mann-Whitney *U* test for each point compared with wtPAX5 luciferase activity ($P < .01$, n = 3).

Results

Cytogenetic characteristics of the cohort

The criterion for inclusion in this retrospective study was the detection on karyotype of acquired structural 9p rearrangement in B-ALL patients. Karyotypes were mostly pseudodiploid (53% children and 52% adults). A total of 32% had a modal number of 45 chromosomes (31% children and 33% adults). Hypodiploid karyotypes with 44 chromosomes were rare, only found in 2 cases. In the hyperdiploid group, modal numbers ranged from 47 to 55. Only 2 cases (1%) with a high hyperdiploid karyotype (> 50 chromosomes) were detected. Details of karyotypes are given in supplemental Table 2.

Karyotype and fluorescence in situ hybridization (FISH) analyses revealed that 14.5% of the patients harbored a t(9;22)(q34;q11)/*BCR-ABL1* (4.5% in children, 28% in adults), 6.5% a t(1;19)(q23;p13)/*TCF3-PBX1* (9% in children, 3% in adults), 9 pediatric cases a t(12;21)(p13;q22)/*ETV6-RUNX1* (10%), 2 cases a 11q23/*MLL* translocation (2% children), and 3.5% a 14q32/*IGH* translocation (2% children and 5% adults).

To assess the distribution and the combination of the most frequent abnormalities associated with the 9p alteration, we reported all the chromosomal changes in Table 1, supplemental Table 3, and supplemental Figure 1. The most frequent abnormalities were in decreasing order: 20q deletion, 12p deletion, 9q translocation different from 9q34/*ABL1*, 13q abnormalities (deletion or translocation), 6q deletion, trisomy 8 or 8q gain, 7p deletion, 11q abnormalities different from 11q23/*MLL*, 7q translocation, 17p deletion, 5q translocation, and high hyperdiploidy.

Complex karyotypes (≥ 3 unrelated chromosomal abnormalities) were frequent, found in 48% (44% children and 54% adults, $P = .3$).

However, the chromosomal abnormalities that rendered these karyotypes complex differed in the 2 age groups. In children, complexity was mainly the result of the contribution of known recurrent changes in B-ALL (12p-, 20q-, 6q-, etc), whereas in adults, complexity mainly resulted from nonrecurrent changes indicating a higher heterogeneity of genome alterations (Table 1; supplemental Table 3; supplemental Figure 1).

The 9p abnormalities found in our cohort were translocations (resulting in 9p deletions when unbalanced), dicentrics, and isochromosome 9q leading to partial or total monosomy 9p, inversions, insertions, and simple deletions. Only a small number of cases of simple deletions were included.

Table 1. Cytogenetic distribution of chromosomal associated abnormalities in total cohort

Cytogenetic subgroup	t(9;22)	t(1;19)	t(12;21)	t(14q32)	t(11q23)	del(20q)	del(12p)	t(9q	abn(13q)	del(6q)	+8/8q	del(7p)	abn(11q)	t(7q)	del(17p)	t(5q)	Breakpoint/ PAX5 Centro	Breakpoint/ PAX5 Intra	Breakpoint/ PAX5 Telo	Complex	High hyper
t(9;22)	**22**	—	—	—	—	—	—	—	—	—	—	—	—	—	—	—	—	—	—	—	—
t(1;19)	—	**10**	—	—	—	—	—	—	—	—	—	—	—	—	—	—	—	—	—	—	—
t(12;21)	—	—	**9**	—	—	—	—	—	—	—	—	—	—	—	—	—	—	—	—	—	—
t(14q32)	—	—	—	**5**	—	—	—	—	—	—	—	—	—	—	—	—	—	—	—	—	—
t(11q23)/MLL	—	—	—	—	**2**	—	—	—	—	—	—	—	—	—	—	—	—	—	—	—	—
del(20q)	1	—	—	—	—	**27**	—	—	—	—	—	—	—	—	—	—	—	—	—	—	—
del(12p)	—	—	5	1	—	—	**21**	—	—	—	—	—	—	—	—	—	—	—	—	—	—
t(9q other than ABL1	—	2	1	—	1	4	2	**21**	—	—	—	—	—	—	—	—	—	—	—	—	—
abn(13q)	1	1	—	—	—	1	4	2	**17**	—	—	—	—	—	—	—	—	—	—	—	—
del(6q)	—	2	3	—	—	1	6	3	5	**13**	—	—	—	—	—	—	—	—	—	—	—
+8/8q	4	—	—	—	—	3	3	—	2	—	**11**	—	—	—	—	—	—	—	—	—	—
del(7p)	2	2	1	1	1	—	—	1	2	—	—	**11**	—	—	—	—	—	—	—	—	—
abn(11q) other than MLL	2	1	2	—	—	2	2	1	3	2	2	1	**10**	—	—	—	—	—	—	—	—
t(7q)	—	—	—	1	—	1	—	1	2	—	—	1	2	**9**	—	—	—	—	—	—	—
del(17p)	1	1	—	—	—	1	—	—	2	1	—	1	—	—	**8**	—	—	—	—	—	—
t(5q)	1	—	1	—	—	—	—	1	—	—	—	1	—	1	1	**8**	—	—	—	—	—
Breakpoint/PAX5																					
Centromeric	20	9	5	4	1	15	9	12	10	7	6	9	7	3	7	3	**92**	—	—	—	—
Intragenic	—	—	—	1	1	9	6	2	1	1	3	1	1	4	1	2	2	**32**	—	—	—
Telomeric	2	1	4	—	—	3	6	7	6	5	2	1	2	2		3	5	2	**29**	—	—
Complex	NA	NA	NA	NA	NA	13	7	12	14	7	6	2	5	3	5	1	30	8	12	**50**	—
High hyper	1	—	—	—	—	—	—	1	—	—	—	—	—	—	—	—	—	—	2	1	**2**

Patients were classified according to the presence of the following chromosomal abnormalities: t(9;22)(q34;q11)/*BCR-ABL1*, t(1;19)(q23;p13)/*TCF3-PBX1*, t(12;21)(p13;q22)/ *ETV6-RUNX1*, 11q23 translocations/*MLL*, 14q32 translocations/*IGH*, and the chromosomal regions most often disrupted in this cohort (≥ 8 patients): 20q deletion, 12p deletion, 9q translocation different from 9q34/*ABL1*, 13q abnormalities (deletion or translocation), 6q deletion, trisomy 8 or 8q gain, 7p deletion, 11q abnormalities different from 11q23/*MLL*, 7q translocation, 17p deletion, 5q translocation, high hyperdiploidy, and complex karyotype, excluding those patients with t(9;22), t(1;19), t(12;21), 14q32/IGH, and 11q23/MLL. For patients with such recurrent translocations, complexity calculation was NA. 9p breakpoint localization was mapped by cytogenetic analysis and was indicated in the table according to *PAX5* probe position (centromeric, telomeric, and intragenic). Therefore, the submicroscopic deletions of *PAX5* exons, not detectable by cytogenetic methods, were not investigated.

— indicates no case; and NA, not applicable.

Various *PAX5* alterations and their association with karyotypic features

All patients were screened with a commercial dual-color *PAX5* probe (Figure 1). When the 2 colors were separated, indicating a possible *PAX5* internal rearrangement, we performed further analyses to pinpoint the location of the breakpoint (Figure 1).

Because our study was based on cytogenetic methods, the submicroscopic intragenic alterations of *PAX5* (limited to a few exons) were not investigated.

PAX5 was not altered (telomeric breakpoint) in 29 cases (19%; 21.5% children and 16% adults, $P = .4$, male/female ratio = 1.2). Complex karyotypes were frequent (54.5%), and the 2 cases of high hyperdiploid karyotypes belonged to this group (Table 1). Only 2 patients had a partial loss of the *PAX5* probe signal. Of the 27 remaining patients, 18 harbored unbalanced 9p rearrangement on the karyotype without losing the *PAX5* probe signal.

Centromeric breakpoints were observed in 92 patients (60%, 54% children and 69% adults, $P = .068$, male/female ratio = 1.5). This 9p rearrangement generated a loss of *PAX5* in 86 patients (93%). The entire *PAX5* locus was translocated onto another chromosome in all other cases. The majority of recurrent fusions found in our cohort belonged to this group: 91% of *BCR-ABL1* (20 of 22), 90% of *TCF3-PBX1* (9 of 10), 80% of *IGH* translocation (4 of 5), 56% of *ETV6-RUNX1* (5 of 9), and 50% of *MLL* translocation (1 of 2). In addition, this group composed 60% of the complex karyotypes (n = 30 of 50; Table 1; supplemental Table 3).

In addition, we detected a breakpoint localized inside the genomic region of *PAX5* resulting in an internal rearrangement of *PAX5* in 32 patients (25% children and 16% adults, $P = .23$, male/female ratio = 1.9). In contrast with the telomeric or centromeric breakpoint cases, a majority of these patients had a simple karyotype (73%, 22 of 30; $P = .024$). Only 2 patients had additional recurrent rearrangement: one case of t(10;14)(p12;q32) implicating the *IGH* locus and another case with *MLL/MLLT3* fusion. Notably, no other recurrent fusion (*BCR-ABL1, TCF3-PBX1,* and *ETV6-RUNX1*) was detected in this group.

PAX5 internal rearrangements showed heterogeneous patterns of breakpoints (Figure 1; supplemental Table 2). The majority of the patients (n = 24) harbored *PAX5* breakpoints located between exon 4, corresponding to the end of the DNA binding domain, and exon 6, coding the homeodomain. This breakpoint position was more frequent in children (19 of 89, 21%) than in adults (5 of 64 cases, 8%; $P = .025$). Furthermore, the *PAX5* telomeric probe signal was deleted for 22 of 24 patients (92%). Among them, 21 of 24 (88%) appeared unbalanced on the karyotype (mainly dicentric and derivative chromosomes), the 3 others had a partial deletion. Three patients (2 adults and 1 male child) harbored breakpoints located in intron 7/intron 8. These patients showed a simple pseudodiploid karyotype and had a balanced rearrangement. Two patients (1 adult and 1 child) harbored a balanced translocation with *PAX5* breakpoint located before the third exon, just before the DNA binding domain. The last 3 cases (2 adult females and 1 female child) showed an unbalanced translocation with breakpoints located in the last 2 exons of *PAX5*.

These results showed that *PAX5* internal rearrangements were not associated with the most common B-ALL recurrent translocations, as these were, most of the time, the sole chromosomal abnormality. On the other hand, *PAX5* deletion was associated with complex karyotypes and classic recurrent translocations.

Frequent alterations of *PAX5* in dicentric chromosomes involving the 9p arm

Childhood and adult cohort presented the same frequency of dicentric rearrangements in 26 of 89 (29%) and 14 of 64 (22%), respectively, $P = .18$. The majority (23 of 40, 58%) resulted in monoallelic deletion of *PAX5* [10 dic,(9;20) 4 dic,(9;12) 5 dic,(7;9) 1 dic, (9;16) 1 dic, (9;17) the dic(8;9), and the dic(9;15)]. Only 5 patients did not delete *PAX5* [3 dic, (9;20) the idic(9;9), and the dic(9;13)], and 12 patients had a *PAX5* intragenic breakpoint associated with partial deletion [4 dic,(9;20) 3 dic, (9;12) 2 dic(9;16), and 2 dic(9;17)] or without deletion of the gene [1 dic(7;9)]. Interestingly, dicentric cases with internal *PAX5* breakpoint were much more frequent in children than in adults (11 of 26 vs 1 of 14 case, $P = .024$). Identical cytogenetic abnormalities proved to result in different genomic breakpoints. Thus, we showed that dicentric rearrangements involving 9p are associated with *PAX5* deletion or internal rearrangement in approximately 90% of cases.

Molecular consequences of *PAX5* internal breakpoints

According to the material available, we could investigate the presence of *PAX5* fusion transcripts in 23 of the 32 patients with internal rearrangement. We identified an in-frame fusion of exon 4 of *PAX5* with exon 3 of *ETV6* by specific reverse-transcribed PCR and confirmed the rearrangement by FISH using *ETV6* probes in 3 cases of dic(9;12)(p13;p13) (#99, #100, and #105; data not shown). The t(7;9)(q11;p13) translocation, which fused exon 7 of *PAX5* to exon 2 of *ELN*, was previously described by our group[11] in 2 of the 3 patients of this cohort (#119, #120). The presence of *PAX5-ELN* was confirmed in the third patient by FISH with *ELN* specific BAC probes (#121; supplemental Figure 2). We also confirmed the presence of known chimeric transcripts in 2 cases of t(3;9)(p14;p13) (#97, #98). This rearrangement yielded a chimeric transcript, which fused in-frame exon 6 of *PAX5* to exon 7 of *FOXP1* in one case (no RNA was available for the second patient). This fusion transcript was detected by RCA-RACE and confirmed by FISH using *FOXP1* specific BAC probes for both (supplemental Figure 2). We detected *PAX5-JAK2* fusion transcript in a del(9)(p13;p24) case (#118). This translocation led to in-frame chimeric transcript, which fused exon 5 of *PAX5* to exon 19 of *JAK2*. The 2 genes being originally in opposite orientation on the 9p arm, we speculated that a deletion occurred before/or concomitant with *JAK2* inversion. In agreement with these data, FISH experiments revealed that the *JAK2* probe signal was slightly decreased whereas the *PAX5* signal kept only the centromeric part of the probe (supplemental Figure 2). We identified the *PAX5-POM121* chimeric transcript in 1 patient with a t(7;9)(q11;p13) (#93). This case expressed an in-frame fusion transcript, which composed the 5 first exons of *PAX5*, 77 noncontiguous nucleotides from *PAX5* intron 5/intron 6, and *POM121* sequence from base 14 of exon 4 (located in the 5′-untranslated region) to the end. The corresponding predicted protein juxtaposed PAX5 N-terminal sequence, included nuclear localization signal (NLS), 72 amino acids, which do not form any predictive structural domain, and the complete POM121 sequence (supplemental Table 4).

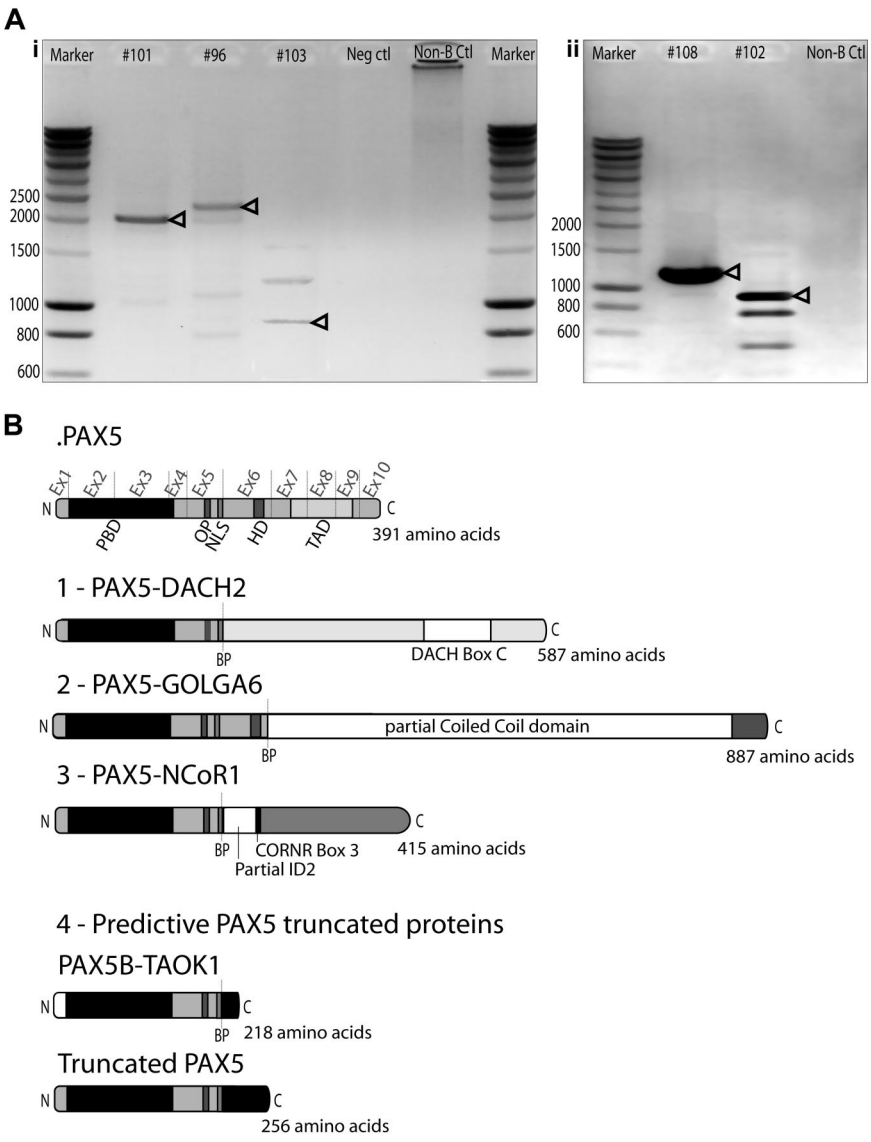

Figure 2. Cloning of novel *PAX5* fusion partners by RCA-RACE. (A) RCA-RACE products were run on 1% agarose gel. Bands corresponding to amplified transcripts of fusion (i) or truncated genes (ii) are indicated by arrowheads. Additional bands correspond to amplification of fragments of wild-type *PAX5* DNA. (i) Patient #101 amplified product corresponds to *PAX5-NCoR1* fusion cDNA, #96 to *PAX5-DACH2* fusion, #103 to *PAX5-GOLGA6* fusion cDNA. (ii) Patient #108 product corresponds to truncated *PAX5* cDNA, #102 to *PAX5-TAOK1* fusion. (B) Schematic illustration of the fusion proteins predicted from cDNA sequencing, breakpoints (BP) are indicated by dashed lines. Ex1-10 indicates *PAX5* exons. All fusion proteins retain the PAX5 DNA-binding domain (PBD, amino acids 16-142), the OP motif (amino acids 179-186), and NLS (amino acids 195-201). (1) PAX5-DACH2 contains the conserved coiled-coil domain of DACH2 (DACH-box C). (2) PAX5-GOLGA6 sequence contains a large part of a predicted coiled-coil domain of GOLGA6. (3) PAX5-NCoR1 retains part of the inhibitor of DNA-binding 2 (ID2) domain and the corepressor-nuclear receptor box 3 (CoRNR box 3). (4) PAX5-TAOK1 predictive protein contains an alternative amino acid sequence encoded by exon1B of *PAX5* and an additional 17-amino acid tail, which does not correspond to any predictive functional domain. Truncated PAX5 contains N-terminal part of PAX5 (amino acids 1-201) and a 55-amino acid tail coded by the contiguous intron 5/intron 6 nucleotide sequence, which does not correspond to any predictive functional domain.

In addition, 3 new *PAX5* rearrangements have been molecularly characterized in this study using RCA-RACE technique (Figure 2). In the chimeric transcript resulting from the t(X;9)(q21;p13) (#96), the exon 5 of *PAX5* was fused in-frame to exon 3 of *Dachshund 2* (*DACH2*). FISH analysis with *DACH2* specific BAC probes was performed and confirmed its involvement in this case (supplemental Figure 2). The t(9;17)(p13;p11) led to generation of a chimeric transcript, which fused exon 5 of *PAX5* in-frame with exon 43 of *Nuclear receptor Co-Repressor 1* (*NCoR1*; #101). We also detected an in-frame fusion between exon 6 of *PAX5* and exon 3 of *golgi autoantigen, golgin subfamily a, 6* (*GOLGA6*) in a case of t(9;15)(p13;q24) translocation (#103).

Five cases led to the production of truncated *PAX5* transcripts. In a t(9;17)(p13;q11) case (#102), *PAX5* was disrupted inside the intron 5/intron 6 and fused to intron 19/intron 20 of *TAO kinase 1* (*TAOK1*) in reverse orientation to its open reading frame. Chimeric *PAX5* transcript conserved exon 1B to exon 5 and an additional coding sequence of 54bp. The 3′-untranslated region of this transcript contained part of intron 19/intron 20 of *TAOK1*. This was further confirmed by FISH using *TAOK1* specific BAC probes. On comparative genomic hybridization-single nucleotide polymorphism (CGH-SNP) chip, biallelic deletion of *PAX5* exon 1A was detected, confirming the absence of PAX5A truncated isoform (supplemental Figure 3). This translocation was associated with an unbalanced t(17;20)(q11;q11), and SNP-CGH array revealed that the locus modified by this latter rearrangement involved an intergenic region. In case #108 with a dic(9;16)(p13;q11), we isolated a truncated *PAX5*, conserving exon 1A to exon 5 and 162 bp of additional coding sequence corresponding to the contiguous intron 5/intron 6 sequence (supplemental Table 4). CGH-SNP array analyses were performed and revealed that partner region on 16q11 did not contain any gene, suggesting that the dic(9;16)(p13;q11) results only in forced expression of the truncated transcript (supplemental Figure 3). This truncated form was also detected in 2 cases (#107, #122, data not shown) for which we could not detect any *PAX5* fusion transcript. CGH-SNP analyses on patient #112 with a dic(9;20)(p13;q11) revealed breakpoints in intron 6/intron 7 of *PAX5* and in the last exon of *Pleiomorphic adenoma gene-like 2* (*PLAGL2*), leading to a putative truncated form of PAX5 (supplemental Figure 3).

Because PAX5 fusion proteins have been shown to act as competitive inhibitor of wtPAX5 transactivation activity,[2,11,17] we assessed the functional consequence of one of the new fusion (PAX5-NCoR1) and of the truncated form (cloned from patient

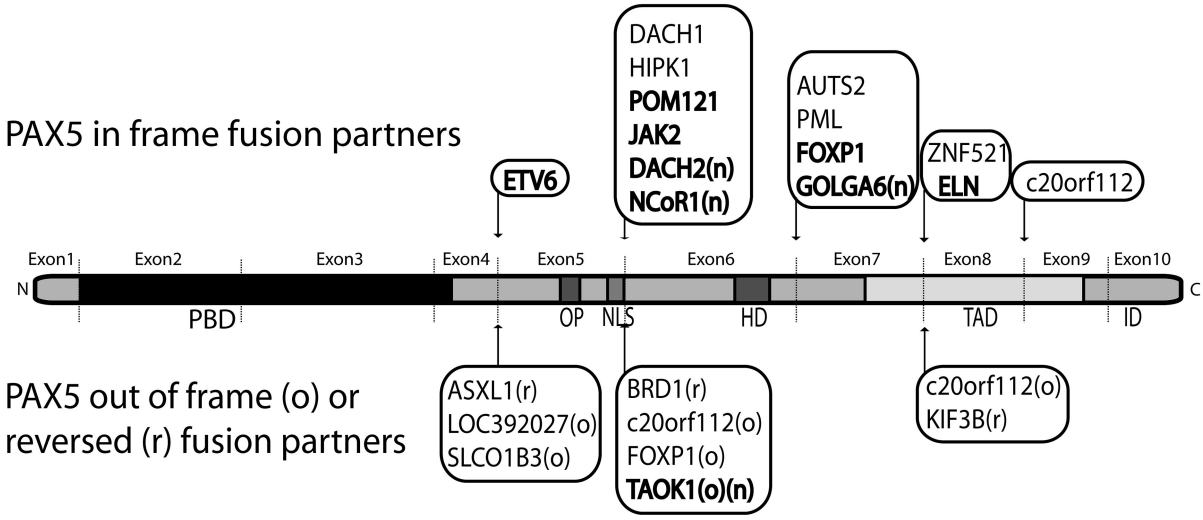

Figure 3. 3′-PAX5 fusion partners in B-ALL. Partners previously described (references in supplemental Table 5) and detected in our series are indicated in bold, new PAX5 fusion partners are highlighted with an "n." In-frame PAX5 fusions are indicated on the upper side. Fusion partners in reverse orientation (r) or out-of-frame fusion (o), leading to PAX5 predictive truncated protein are indicated on the lower side. PBD, OP, NLS, homeodomain (HD), transactivation domain (TAD), and inhibitory domain (ID) are shown.

#108) using a luciferase reporter assay.[16]We showed that these 2 types of PAX5 alterations (fusion and truncated form) behaved as competitive inhibitors of wild-type PAX5 transactivating activity (supplemental Figure 4).

In summary, we detected 5 recurrent and 3 new partner genes, thus confirming the wide diversity of *PAX5* fusion partners. We also showed that truncated PAX5 can be a recurrent consequence of different chromosomal translocations.

Discussion

We investigated *PAX5* alterations in a large cohort of 153 adult and childhood B-ALL patients harboring a 9p abnormality, using classic and innovative molecular and cytogenetic techniques. We detected *PAX5* alteration in 81% of the patients with structural abnormality of the short arm of chromosome 9. Internal rearrangements were found in 21% of the cases, this alteration being significantly associated with simple karyotypes. Furthermore, *PAX5* internal rearrangements and most recurrent translocations commonly found in B-ALL appeared to be mutually exclusive. This implies that *PAX5* internal rearrangement might be sufficient to initiate leukemogenesis, through blockage of B-cell differentiation. Mechanistically, this hypothesis is emphasized by the fact that at least PAX5-ELN,[11] PAX5-FOXP1,[2] and PAX5-ETV6[17] have a trans-dominant negative effect on normal PAX5.

To identify *PAX5* fusion partners, we implemented a new molecular biology method, until now only used in plant biology.[15] The strategy is based on RCA to generate concatenated cDNA containing multiple copies of the target gene. This concatenated cDNA is subsequently used as a template for inverse PCR with 2 specific primers of the known part of the chimera (see principle in supplemental Figure 5). Thus, we isolated additional cases of rare translocations, as described previously (Figure 3). For example, *PAX5-POM121* generated by the t(7;9)(q11;p13) translocation can now be classified as recurrent because we added a second case to a translocation.[9] However, the fusion sequence we described is slightly different from that reported, even though the predictive protein structures are similar. It is noteworthy that the same fusion partner can give rise to either in-frame or out-of-frame chimeric transcripts (eg, *PAX5-FOXP1*).[2,18] The *PAX5* internal breakpoint can also lead to the production of truncated proteins resulting from an out-of-frame fusion (*PAX5-FOXP1*), fusion with a gene in opposite orientation (*PAX5-TAOK1*), or fusion with noncoding sequences. In most instances, a premature stop codon is generated immediately after *PAX5* exon 5. The predicted chimeric proteins conserved the PBD, octapeptide (OP), and NLS of PAX5 (breakpoint after exon 5), suggesting that the chimera is located in the nucleus and able to bind PAX5 targets. It is probable that these truncated PAX5-X proteins block B-cell differentiation in a dominant negative manner, similarly to that reported for other *PAX5* fusion products.[2,11,17]

In addition, the RCA-RACE approach enabled us to clone new fusion genes: *PAX5-NCoR1, PAX5-DACH2*, and *PAX5-GOLGA6* increasing the total number of partners of PAX5 in B-ALL to 20 (Figure 3). *NCoR1* is a component of histone deacetylase complexes and acts as transcriptional repressor by modulating chromatin, which impedes the accessibility of basal transcription factors to genomic regulation sites.[19] Interestingly, NCoR1 partial inhibitor of DNA-binding 2 domain replaces the trans-activating domain of PAX5 and the putative protein may act as a constitutive repressor of PAX5 targets. DACH2 is a transcription factor implicated in organogenesis and is supposed to be involved in proliferation, notably by repressing cyclin-dependent kinase inhibitor expression.[20] As the patient harboring the t(X;9) translocation was a male, the *DACH2-PAX5* fusion is associated with a total loss of wild-type *DACH2*. Moreover, *DACH1*, structurally close to *DACH2*, has been found fused to *PAX5* in a t(9;13)(p13;q22).[9] These results strongly suggest that *DACH* family genes could be involved in oncogenesis. The third in-frame fusion led to the expression of *PAX5-GOLGA6* transcript. *GOLGA6* is highly expressed in human testis, but its function is still unknown.[21]

Remarkably, even if the nature of the partners is very variable, 19 of 23 of the predicted chimeric proteins conserved the PBD, OP motif, and the nuclear localization signal of PAX5 (breakpoint after exon 5), strongly suggesting functional selection of the chimera.

Our data showed that 60% of the patients (adults and children) harbored a monoallelic deletion of *PAX5*. These patients mainly

displayed a complex karyotype and classic recurrent fusion genes (*BCR-ABL1, TCF3-PBX1, ETV6-RUNX1*, and *MLL* rearrangements). We assumed that the complexity of karyotypes in patients with *PAX5* deletion reflects the secondary nature of this event, contrary to internal *PAX5* translocations. Miller et al[22] have recently shown the interplay between *BCR-ABL1* and the deletion of both *PAX5* and *INK4a/ARF* in the leukemia process. Thus, the deletion of *PAX5* might occur concomitantly with the loss of *INK4a/ARF* locus located in 9p21.

Dicentric cases represented 26% of the 9p abnormality, most often involving chromosomes 20, 12, and 7 and frequently leading to the deletion of *PAX5*. We observed that *PAX5* internal rearrangements in dicentric chromosomes were much more frequent in children than in adults. Concerning the dic(9;12) cases, Heerema et al have reported one group of patients harboring *PAX5-ETV6* fusion and another group of patients with both *ETV6-RUNX1* rearrangement and *PAX5* deletion, the 2 groups being mutually exclusive.[23] We characterized a new situation in which patients harbored a *PAX5* deletion without *ETV6-RUNX1* fusion (cases #19, #20, and #106). We assumed that simple karyotypes with dicentric chromosomes are cytogenetic entities with heterogeneous breakpoints. Contrary to *PAX5-ETV6* in the dic(9;12) rearrangement, Strefford et al have suggested that the dic(9;20) are not associated with an identical recurrent gene rearrangement.[24] Our additional cases are in line with this assumption. Interestingly, we noted that dicentric cases can be masked by a complex rearrangement. Two dicentric rearrangements in this series (#101 and #107) involved a third chromosome (17 and 16, respectively). This third partner chromosome was split between chromosome 9 and chromosome 20, without loss of material. The final result was a loss of 9p and 20q in these 2 patients who could be structurally comparable with a dic(9;20).

In conclusion, we showed that *PAX5* was altered in 81% of the cases with a 9p abnormality. These alterations were diverse in terms of nature and associated karyotypic features. The different types of alterations seemed to act at different levels of the leukemia process: *PAX5* internal breakpoints, leading to the expression of fusion proteins or PAX5 truncated proteins, might occur early in the process, by way of contrast, deletions of *PAX5*, which were much more frequent, might appear later in the oncogenic process and could be a secondary event occurring in a cell already undergoing transformation. It is worth noting that *PAX5* chimeric transcripts shared common features regardless of the fusion partners. The majority retained the DNA-binding domain and the NLS of PAX5, strongly suggesting that they may modulate wild-type protein activity in a dominant negative manner. Nonetheless, partner gene impact on leukemogenesis requires further investigation. It would be interesting to determine whether fusion partners are randomly or functionally selected because, to date, it has been impossible to identify features common to all fusion partners.

Acknowledgments

The authors thank Eric Delabesse, Estelle Espinos, and José Meija for fruitful discussions; Roland Heilig and Gabor Gyapay (CNS, Evry, France) for kindly providing the BACs; Prof Meinrad Busslinger for kindly providing the *luc-CD19* reporter plasmid; and the tumor bank of CHU Bordeaux, Bernardine Favre, Patrick Callier, Nathalie Marle (CRB Centre Hospitalier Universitaire Dijon), and Barbara De Moerloose (Department of Pediatric Hemato-Oncology, Ghent University Hospital, Ghent, Belgium) for technical support.

This work was supported by the Institut National du Cancer, Laurette Fugain foundation, the Cooperación de investigation transpirenaica en la terapia innovadora de la leukemia, the Recherche et Innovation en Thérapeutique Cancéreuse, Fondation de France, and l'association pour la recherche sur le Cancer (no. 4841).

Authorship

Contribution: C. Broccardo, N.D., and P.B. designed the study, C. Broccardo, E.C., S.S., N.D., and P.B. wrote the paper; E.C., S.S., N.P., J.F., R.E., C.Q., and M.B. performed the research and analyzed the data; and N.D., F.M., P.T., M.-P.P., C.L., D.P., E.L., N.N., S.T., B.P., I.L., L.B., V.E., I.R., C. Barin, M.-J.M., M.L.-P., H.A.-P., C.C., C.P., and C.T. provided patient samples, performed the karyotype analyses, and gave critical suggestions.

Conflict-of-interest disclosure: The authors declare no competing financial interests.

Correspondence: Cyril Broccardo, Inserm U563, CHU Purpan, CPTP BatB, BP3028, 31024 Toulouse Cedex 3, France; e-mail: cyril.broccardo@inserm.fr.

References

1. Armstrong SA, Look AT. Molecular genetics of acute lymphoblastic leukemia. *J Clin Oncol.* 2005;23(26):6306-6315.
2. Mullighan CG, Goorha S, Radtke I, et al. Genome-wide analysis of genetic alterations in acute lymphoblastic leukaemia. *Nature.* 2007; 446(7137):758-764.
3. Familiades J, Bousquet M, Lafage-Pochitaloff M, et al. PAX5 mutations occur frequently in adult B-cell progenitor acute lymphoblastic leukemia and PAX5 haploinsufficiency is associated with BCR-ABL1 and TCF3-PBX1 fusion genes: a GRAALL study. *Leukemia.* 2009;23(11):1989-1998.
4. Nutt SL, Heavey B, Rolink AG, Busslinger M. Commitment to the B-lymphoid lineage depends on the transcription factor Pax5. *Nature.* 1999; 401(6753):556-562.
5. Cobaleda C, Jochum W, Busslinger M. Conversion of mature B cells into T cells by dedifferentiation to uncommitted progenitors. *Nature.* 2007; 449(7161):473-477.
6. Delogu A, Schebesta A, Sun Q, Aschenbrenner K, Perlot T, Busslinger M. Gene repression by Pax5 in B cells is essential for blood cell homeostasis and is reversed in plasma cells. *Immunity.* 2006;24(3):269-281.
7. Schebesta A, McManus S, Salvagiotto G, Delogu A, Busslinger GA, Busslinger M. Transcription factor Pax5 activates the chromatin of key genes involved in B cell signaling, adhesion, migration, and immune function. *Immunity.* 2007;27(1):49-63.
8. Cazzaniga G, Daniotti M, Tosi S, et al. The paired box domain gene PAX5 is fused to ETV6/TEL in an acute lymphoblastic leukemia case. *Cancer Res.* 2001;61(12):4666-4670.
9. Nebral K, Denk D, Attarbaschi A, et al. Incidence and diversity of PAX5 fusion genes in childhood acute lymphoblastic leukemia. *Leukemia.* 2009; 23(1):134-143.
10. An Q, Wright SL, Konn ZJ, et al. Variable breakpoints target PAX5 in patients with dicentric chromosomes: a model for the basis of unbalanced translocations in cancer. *Proc Natl Acad Sci U S A.* 2008;105(44):17050-17054.
11. Bousquet M, Broccardo C, Quelen C, et al. A novel PAX5-ELN fusion protein identified in B-cell acute lymphoblastic leukemia acts as a dominant negative on wild-type PAX5. *Blood.* 2007;109(8): 3417-3423.
12. Heerema NA, Sather HN, Sensel MG, et al. Association of chromosome arm 9p abnormalities with adverse risk in childhood acute lymphoblastic leukemia: a report from the Children's Cancer Group. *Blood.* 1999;94(5):1537-1544.
13. Bene MC, Castoldi G, Knapp W, et al. Proposals for the immunological classification of acute leukemias: European Group for the Immunological Characterization of Leukemias (EGIL). *Leukemia.* 1995;9(10):1783-1786.
14. Shaffer L, Tommerup N. *An International System for Human Cytogenetic Nomenclature.* Basel, Switzerland: Karger; 2005;1-130.
15. Polidoros AN, Pasentsis K, Tsaftaris AS. Rolling

circle amplification-RACE: a method for simultaneous isolation of 5′ and 3′ cDNA ends from amplified cDNA templates. *Biotechniques.* 2006; 41(1):35-36.

16. Dörfler P, Busslinger M. C-terminal activating and inhibitory domains determine the transactivation potential of BSAP (Pax-5), Pax-2 and Pax-8. *EMBO J.* 1996;15(8):1971-1982.
17. Fazio G, Palmi C, Rolink A, Biondi A, Cazzaniga G. PAX5/TEL acts as a transcriptional repressor causing down-modulation of CD19, enhances migration to CXCL12, and confers survival advantage in pre-BI cells. *Cancer Res.* 2008;68(1): 181-189.
18. Kawamata N, Ogawa S, Zimmermann M, et al. Cloning of genes involved in chromosomal translocations by high-resolution single nucleotide polymorphism genomic microarray. *Proc Natl Acad Sci U S A.* 2008;105(33):11921-11926.
19. Hörlein AJ, Naar AM, Heinzel T, et al. Ligand-independent repression by the thyroid hormone receptor mediated by a nuclear receptor co-repressor. *Nature.* 1995;377(6548):397-404.
20. Davis RJ, Shen W, Sandler YI, Heanue TA, Mardon G. Characterization of mouse Dach2, a homologue of Drosophila dachshund. *Mech Dev.* 2001;102(1):169-179.
21. Gilles F, Goy A, Remache Y, Manova K, Zelenetz AD. Cloning and characterization of a Golgin-related gene from the large-scale polymorphism linked to the PML gene. *Genomics.* 2000;70(3): 364-374.
22. Miller CB, Mullighan CG, Su X, et al. Pax5 haploinsufficiency cooperates with BCR-ABL1 to induce acute lymphoblastic leukemia [Abstract]. *Blood (ASH Annual Meeting Abstracts).* 2008; 112:Abstract 293.
23. Heerema NA, Raimondi SC, Anderson JR, et al. Specific extra chromosomes occur in a modal number dependent pattern in pediatric acute lymphoblastic leukemia. *Genes Chromosomes Cancer.* 2007;46(7):684-693.
24. Strefford JC, Worley H, Barber K, et al. Genome complexity in acute lymphoblastic leukemia is revealed by array-based comparative genomic hybridization. *Oncogene.* 2007;26(29):4306-4318.